33rd Annual International Conference of the IEEE EMBS
Boston, Massachusetts USA, August 30 - September 3, 2011

CARES 3.0: A Two Stage System combining Feature-Based Recognition and Edge-based Segmentation for CIMT Measurement on a Multi-Institutional Ultrasound Database of 300 images

Filippo Molinari, *Member, IEEE*, Kristen M. Meiburger, *Graduate Student Member, IEEE*, U. Rajendra Acharya, *Member Sr. IEEE*, Guang Zeng, Paulo S. Rodrigues, Luca Saba, Andrew Nicolaides, and Jasjit S. Suri, *Fellow AIMBE, Senior Member, IEEE*

***Abstract*—The intima-media thickness of the carotid artery (CIMT) is a validated marker of atherosclerosis. Accurate CIMT measurement can be performed by specifically designed computer algorithms. We improved a previous CIMT measurement technique by introducing a smart heuristic search for the lumen-intima (LI) and media-adventitia (MA) interfaces of the carotid distal wall. We called this new release as CARES 3.0 (a class of AtheroEdge™ system, a patented technology from Global Biomedical Technologies, Inc., CA, USA). CARES 3.0 is completely automated and adopts an integrated approach for carotid location in the image frame, followed by segmentation based on edge snapper and heuristic search. CARES 3.0 was benchmarked against three other techniques on a 300 image multi-institutional database. One of the techniques was user-driven. The CARES 3.0 CIMT measurement bias was -0.021±0.182 mm, which was better than that of the semi automated method (-0.036±0.183 mm). CARES 3.0 outperformed the other two fully automated methods. The Figure-of-Merit of CARES 3.0 was 97.4%, better than that of the semi-automated technique (95.4%).**

I. Introduction

The carotid artery (CA) thickening is one of the earliest markers of increased risk of cardiovascular diseases. Several large studies and international consensuses, showed that the carotid artery intima – media thickness (CIMT) is a reliable marker of atherosclerosis [1].

In clinical practice, trained and certified sonographers manually measure the CIMT in ultrasound longitudinal projections of the CA. Manual measurement is time consuming, operator-dependent, and prone to errors and inaccuracies. Computer-based algorithms are now widely used to aid and improve the CIMT measurement.

CIMT measurement techniques can be divided into semi-automated and fully automated. In a recent review, Molinari *et al.* described the most widely used and performing techniques for CIMT measurement [2].

We recently proposed an automated CIMT measurement technique called CARES (Completely Automated and Robust Edge Snapper) [3] (a class of AtheroEdge™ system from Global Biomedical Technologies, Inc., CA, USA). CARES used an integrated approach to locate the carotid artery in the image frame and an edge snapper to perform wall segmentation and recognition of the lumen-intima (LI) and media-adventitia (MA) transitions. However, performance was unsatisfactory in terms of CIMT reproducibility of the technique. In this paper, we show a new and improved third-generation of this segmentation strategy, called CARES 3.0. We benchmarked CARES 3.0 on a 300 image database coming from two Institutions against one semi-automated technique and two fully automated algorithms.

II. CARES 3.0 Segmentation Architecture

A. Stage-I: Automated Carotid Recognition

Stage-I consists in the automated localization of the carotid artery in the image frame, giving forth an automated tracing of the far adventitial profile (AD_F). We used a technique called CALEX which is based on an integrated approach consisting in (*a*) feature extraction, (*b*) fitting, and (*c*) validation, which we had previously developed and published [4, 5]. The first version of the architecture has been improved by inserting two major controls, which improve the accuracy of the AD_F tracing (CALEX 3.0).

1) Artery Lumen Automated Detection

The lumen can be automatically detected by looking at the pixels' neighborhood. Lumen pixels have a neighborhood with a low mean intensity and a low standard deviation. Our strategy consisted in computing the average values and the standard deviations for all the pixels and then building a bi-dimensional normalized histogram. All the pixels having a neighborhood (10x10) intensity value lower than 0.08 and a standard deviation lower than 0.14 were considered as belonging to the artery lumen [6].

2) Spike Detection and Removal

We ran a spike detection and removal procedure that deleted every glitch in the AD_F profile with amplitude higher that 10 pixels, which is about 60% the size of the CIMT expressed in pixels.

F. Molinari and K.M. Meiburger are with the BioLab, Department of Electronics, Politecnico di Torino, Torino, Italy (Corresponding Author; phone: +39-11-564-4135; fax: +39-11-564-4217; e-mail: filippo.molinari@polito.it).

U.R. Acharya is with the Dept ECE, Ngee Ann Polytechnic, Singapore

G. Zeng is with Mayo Clinic, Rochester, MN, USA.

P. S. Rodrigues is with Department of Computer Science, Centro Universitário da FEI, São Paulo, Brazil.

L. Saba is with the Dept. of Radiology, A.U.O. Cagliari, Italy.

A. Nicolaides is with the Vascular Screening Diagnostic Center, Nicosia, Cyprus.

J.S. Suri is CTO of Global Biomedical Technologies, Inc., Roseville, CA, USA and (Aff.) Idaho State University, Pocatello, ID, USA (jsuri@comcast.net).

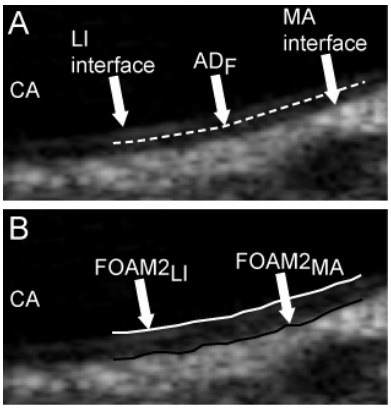

Fig. 1. A) Sample of AD_F tracing in-between LI/MA. B) Demonstration of correct LI/MA segmentation by modified FOAM (called FOAM2 in the image).

B. Stage-II: Domain based LI/MA Segmentation Strategy

Stage-II is devoted to the automated LI/MA boundaries tracing. We focus the LI/MA tracing in a region of interest (ROI) or guidance zone (GZ). Overall, Stage-II consists of four cascaded steps.

First of all, we built a region-of-interest (ROI) or guidance zone (GZ) around the automatically traced *far adventitia* AD_F profile, with a horizontal length equal to the length of the AD_F and a height equal to 30 pixels.

1) Edge Enhancement by FOAM operator

We used the ***F**irst **O**rder **A**bsolute **M**oment* (FOAM) operator for improving the LI/MA edges representation in the automatically designed guidance zone [7]. We used the implementation as proposed by Faita *et al.* [8]. Considering an Image *I(x,y)*, the FOAM operator can be expressed as:

$$e(x,y) = \int_{\theta_2} \left| I_1(x,y) - I_2(x-k,y-l) \right| \cdot G(k,l,\sigma_3)\, dk\, dl \quad (1)$$

where, $I_1(x,y)$ and $I_2(x,y)$ correspond to the original image *I(x,y)* after filtering by a Gaussian Kernel with parameter equal to σ_1 and σ_2, respectively. The Gaussian Kernel $G(x,y,\sigma_3)$ is a third kernel used for smoothing the FOAM operator *e(x,y)*. FOAM is an edge-map that has a value close to zero in homogeneous regions (*i.e.* in regions without intensity changes and that are of the same gray level), and reaches a maximum when computed in proximity of an intensity gradient. Gemignani *et al.* [9] suggested using all the σ values equal to 1/3rd of the kernel size. We used a kernel size of 5 pixels for the $G(x,y,\sigma_1)$ and $G(x,y,\sigma_3)$, and of 10 pixels for $G(x,y,\sigma_2)$. Consequently, we took $\sigma_1 = \sigma_3 = 2$ pixels and $\sigma_2 = 3$ pixels.

2) Heuristic Search for the LI/MA peaks

We first ran the lumen detection on the GZ, to avoid LI jumping into the carotid lumen. The heuristic search was then structured as:

1. We identified all the intensity maxima of the intensity profile, which were comprised into the first 75-th percentile of the intensity distribution of the FOAM column under analysis, avoiding lumen points.
2. The intensity profile was scanned from the lumen to the adventitia. The first intensity maximum that had intensity in the 75-th percentile and was not in the lumen region was marked as a LI candidate point.
3. We kept all the intensity maxima that were comprised into the first 90-th percentile of the intensity distribution of the FOAM column, considered between the LI point and the adventitia point (*i.e.* the point corresponding to the AD_F profile). The closest maximum to LI was marked as a MA candidate point.
4. We repeated the process for all the columns of the image and the sequence of the LI and MA candidate points formed the LI/MA boundaries.

3) LI/MA Regularization and Error Check

Figure **1.A** shows a condition possibly leading to an error in the MA detection. The AD_F was traced in-between the LI/MA profiles. Since the intensity of the MA interface is usually higher than that of the LI, called $FOAM_{LI}^{i}$ and $FOAM_{MA}^{i}$ the FOAM intensity of the LI and MA candidate points relative to the *i-th* column. If we found that $FOAM_{LI}^{i} > FOAM_{MA}^{i}$, then we assumed that the MA candidate point was a false candidate. Hence, we extended the guidance zone 8 pixels towards the bottom of the image and repeated the heuristic search starting from step **3)**. If the MA detection resulted again in a point with intensity lower than the LI candidate, then the column was discarded. Figure **1.B** demonstrates that the LI/MA boundaries were correctly traced.

Another improvement was given by introducing an adaptive threshold: we first ran our heuristic search by using the 75-th percentile as an intensity criterion for assigning the LI candidate. Let N be the total number of columns of GZ and let N_{LI} be the number of LI candidate points at the end of the heuristic search. If we found $N_{LI} < 0.1\ N$ we decreased the intensity criterion and ran the heuristic once again. The procedure was iterated until $N_{LI} > 0.1\ N$. Finally, spike detection and removal was applied to the LI/MA profiles.

When used as standalone, this peak detection paradigm was called as FOAM 2.0 and required user interaction for the GZ definition. When combined with the previously described Stage-I, however, this technique became automated and was called CARES 3.0.

III. CALEX 3.0 SYSTEM IMPROVEMENT

The typical far-wall identification errors of CALEX 1.0 were when:

(1) Selected line segments were found along the jugular vein above the common carotid artery.

(2) The whole (or part of the) selected line segments deviated from the adventitia layer of the far wall of CCA.

The first error can be fixed by observing that when the line segment is traced on the JV instead of the AD_F, its upper side is brighter than its lower side, while it should be the opposite. We introduced a new feature, called *isadf*, which helps fix the first error by ignoring all the line segments with

an *isadf* value less than a predefined threshold value, $isadf_T$ (= 1.25). For each valid line segment, the *isadf* feature is calculated as:

$$isadf = \frac{\sum_{i=0}^{N}\sum_{j=0}^{M} I(x_i, y_i - j)}{\sum_{i=0}^{N}\sum_{j=0}^{M} I(x_i, y_i + j)}$$

where N is the number of points on the line segment, M (= 30 pixel) is the sample distance, and I is the input image.

The second error was fixed by a refinement procedure. For each point p on the detected far-wall adventitia, we extracted the column intensity profile. We computed the position of the nearest local maximum q and if the intensity difference between p and q was not sufficiently high, the point p was discarded. Fig. 2. shows the initial CALEX 1.0 AD_F profile and the refinement made by CALEX 3.0.

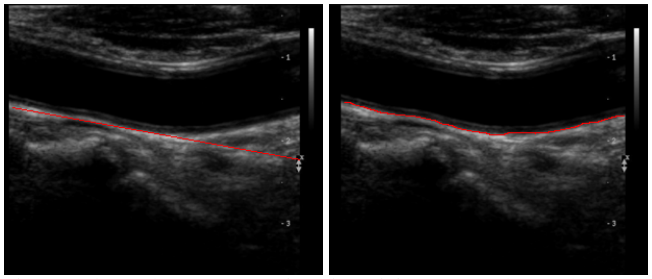

Fig. 2. *Left panel*: CALEX 1.0 detection of the AD_F. *Right panel*: CALEX 3.0 refined and optimized AD_F profile.

IV. Image Database and Benchmarking

We tested CARES 3.0 on a two-institutional database of 300 carotid images. One hundred images were acquired by the Neurology Division of Nicosia (Cyprus) from 100 healthy subjects (age: 54±24, 60 males) with a ATL HDI3000 device (linear probe, recording frequency of 10 MHz, wavelength equal to 155 μm) and 200 from the Neurology Dept. of the Gradenigo Hospital of Torino (Italy) from 150 patients (age: 69±16, 97 males) with a ATL HDI5000 device (linear probe, recording frequency of 7 MHz, wavelength equal to 0.22 mm). The conversion factor for Nicosia images was 0.06 mm/pixel; that of Torino was 0.0625 mm/pixel. Three expert sonographers manually segmented the images and the average profile was considered as ground-truth (the inter-observer variance was found to be equal to 0.0156 pixels).

We benchmarked CARES 3.0 against the user-driven technique, FOAM, by Faita *et al.* [8], which we called FOAM 2.0, and against CALEX 3.0 [5], which has Stage-I in common with CARES 3.0 but a different Stage-II, based on fuzzy *K*-means classification. Also, we benchmarked CARES 3.0 with the previous release of CARES, called CARES 1.0, which has the same Stage-I, but uses FOAM 1.0 in Stage-II, as originally proposed by Faita *et al.* [3]. Both CARES 1.0 and CALEX 3.0 are fully automated techniques. The IMT was calculated as the polyline distance between the LI and the MA boundaries.

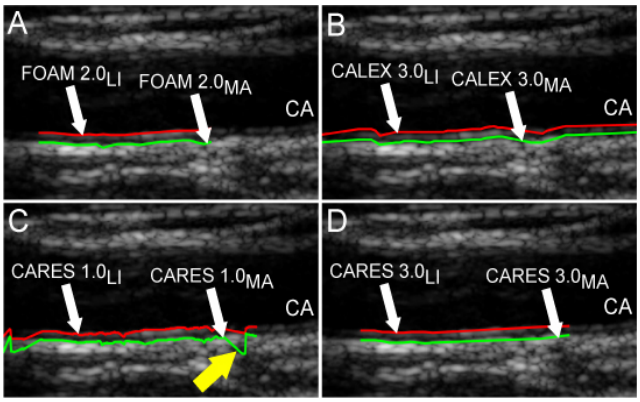

Fig. 3. LI/MA profiles of the four techniques A) FOAM 2.0; B) CALEX 3.0; C) CARES 1.0; D) CARES 3.0. The LI boundary is depicted in red, the MA in green. The yellow arrow in panel C) indicates spikes that have not been corrected in CARES 1.0 profiles. (Color figure)

V. Results and Discussion

Stage-I was successful on 300 out of 300 images (100% success). Fig. 3 reports a sample of carotid distal wall segmentation and LI/MA tracings by FOAM 2.0 (fig. 3.A), CALEX 3.0 (fig. 3.B), CARES 1.0 (fig. 3.C), and CARES 3.0 (fig. 3.D).

A. Far Wall Segmentation and Performance

Table I reports the average CIMT segmentation measurement bias, calculated as the difference between the automated technique IMT measurement and the GT IMT measurement (second column), and the mean squared error (ε^2) for the four techniques. CARES 3.0 showed the best accuracy with a CIMT measurement error equal to -0.021 mm and a ε^2 value of 0.033 mm^2. CARES 3.0 performed better than FOAM 2.0, which showed a CIMT bias of -0.036 mm and a ε^2 of 0.035 mm^2. The difference in ε^2 and in the CIMT bias between CARES 3.0 and FOAM 2.0 was not statistically different (*Student's t-test, $p > 0.5$*). CALEX 3.0 and CARES 1.0 showed a CIMT bias of 0.047 mm and -0.130 mm, respectively. Hence, compared to CARES 1.0, this new architecture of CARES 3.0 showed an accuracy improvement equal to 84%.

TABLE I – CIMT MEASUREMENT BIAS FOR THE FOUR TECHNIQUES

Techniques	CIMT bias (mm)	CIMT □ (mm^2)
FOAM2.0	-0.036±0.183	0.035±0.086
CALEX3.0	0.047±0.297	0.090±0.234
CARES1.0	-0.130±0.330	0.125±0.863
CARES3.0	-0.021±0.182	0.033±0.093

FOAM 2.0, the user-driven method we tested, showed the best reproducibility of 0.183 mm and 0.086 mm^2 for the CIMT bias and ε^2, respectively. CARES 3.0 showed a reproducibility of 0.182 mm and 0.093 mm^2, which were not statistically different from the values of FOAM 2.0 ($p > 0.5$). The reproducibility of CALEX 3.0 and CARES 1.0

were too low for a clinical use. Compared to CARES 1.0, the reproducibility of CARES 3.0 improved by about 45%.

The best performing technique we could find in literature was the FOAM method as originally proposed by Faita *et al.* (FOAM 1.0) [8], which showed a CIMT bias of 0.010 ± 0.038 mm. FOAM was, however, tested on a single-institutional database. On our database, we found that FOAM performance was not satisfactory.

B. CIMT values

Another method of describing the quality of the CIMT measurement is the Figure-of-Merit (FoM). With GT_{CIMT} being the average CIMT value obtained by manual measurements on the entire database, and $CARES3_{CIMT}$ the corresponding value obtained by the CARES 3.0 measurement, we can define the FoM as:

$$FoM_{CARES3} = 100 - \frac{|CARES3_{CIMT} - GT_{CIMT}|}{GT_{CIMT}} \cdot 100 \cdot$$

Similarly, we defined the FoM for the other three techniques. Table II reports the average CIMT values of the four techniques and of the GT measurements (second column). The corresponding FoM values are reported in the third column. CARES 3.0 showed the best FoM equal to 97.4%, followed by the semi-automated FOAM 2.0 that showed a FoM of 95.4%. Compared to CARES 1.0, this new version of CARES 3.0 improved the FoM by 14%.

TABLE II – CIMT VALUES AND FIGURE OF MERIT (FOM)

Techniques	CIMT value (mm)	FoM
FOAM2.0	0.760±0.179	95.4 %
CALEX3.0	0.844±0.255	93.9 %
CARES1.0	0.656±0.288	83.4 %
CARES3.0	0.775±0.210	97.4 %
Ground-Truth	0.796±0.264	-

Fig. 4 reports the Bland-Altmann plots for the four techniques. It can be noticed that CARES 3.0 (fig. 4.D) showed a similar performance to the user-driven FOAM 2.0 (fig. 4.A). The points' dispersion of CALEX 2.0 (fig. 4.B) and CARES 1.0 (fig. 4.C) was higher, denoting a limited CIMT estimation reliability. Due to the improvements in Stage-I and Stage-II (AD_F check and refinement, lumen check, adaptive threshold, and spike removal), CARES 3.0 proved to be more stable and accurate than the other benchmark techniques.

VI. CONCLUSION AND FUTURE PERSPECTIVES

We developed an improved fully automated technique for CIMT measurement in longitudinal ultrasound images. This new version called CARES 3.0 consisted of a new heuristic search for LI/MA detection, which showed high accuracy and reproducibility in CIMT measurement. We compared CARES 3.0 with two other automated techniques and with a semi-automated one. The system performance of CARES 3.0 was equal to that of the user-driven technique and comparable to that of the best performing user-dependent techniques proposed in literature. We are now extensively testing CARES 3.0 in a clinical environment with the aim of using this automated technique for large clinical studies.

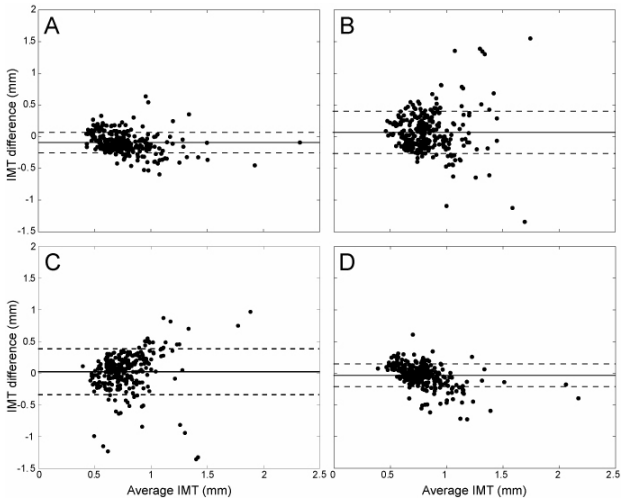

Fig. 4. Bland-Altmann plots for the four techniques. A) FOAM 2.0. B) CALEX 3.0. C) CARES 1.0. D) CARES 3.0.

REFERENCES

[1] P. J. Touboul, M. G. Hennerici, S. Meairs *et al.*, "Mannheim carotid intima-media thickness consensus (2004-2006). An update on behalf of the Advisory Board of the 3rd and 4th Watching the Risk Symposium, 13th and 15th European Stroke Conferences, Mannheim, Germany, 2004, and Brussels, Belgium, 2006," *Cerebrovasc Dis,* vol. 23, no. 1, pp. 75-80, 2007.

[2] F. Molinari, G. Zeng, and J. S. Suri, "A state of the art review on intima-media thickness (IMT) measurement and wall segmentation techniques for carotid ultrasound," *Computer Methods and Programs in Biomedicine,* vol. 100, pp. 201-221, 2010.

[3] F. Molinari, R. U. Acharya, G. Zeng *et al.*, "CARES: Completely Automated Robust Edge Snapper for Carotid Ultrasound IMT measurement on a Multi-Institutional Database of 300 Images: a Two-Stage System Combining An Intensity-Based Feature Approach With First Order Absolute Moments," in SPIE Medical Imaging, Lake Buena Vista (Orlando), Florida, USA, 2011 (accepted).

[4] F. Molinari, G. Zeng, and J. S. Suri, "An integrated approach to computer- based automated tracing and its validation for 200 common carotid arterial wall ultrasound images: A new technique," *J Ultras Med,* vol. 29, pp. 399-418, 2010.

[5] F. Molinari, G. Zeng, and J. S. Suri, "Intima-media thickness: setting a standard for completely automated method for ultrasound," *IEEE Transaction on Ultrasonics Ferroelectrics and Frequency Control,* vol. 57, no. 5, pp. 1112-1124, 2010.

[6] F. Molinari, W. Liboni, P. Giustetto *et al.*, "Automatic computer-based tracings (ACT) in longitudinal 2-D ultrasound images using different scanners," *Journal of Mechanics in Medicine and Biology,* vol. 9, no. 4, pp. 481-505, 2009.

[7] M. Demi, M. Paterni, and A. Benassi, "The first absolute central moment in low-level image processing," *Computer Vision and Image Understanding,* vol. 80, no. 1, pp. 57-87, OCT, 2000.

[8] F. Faita, V. Gemignani, E. Bianchini *et al.*, "Real-time measurement system for evaluation of the carotid intima-media thickness with a robust edge operator," *J Ultrasound Med,* vol. 27, no. 9, pp. 1353-61, Sep, 2008.

[9] V. Gemignani, F. Faita, L. Ghiadoni *et al.*, "A system for real-time measurement of the brachial artery diameter in B-mode ultrasound images," *IEEE Trans Med Imaging,* vol. 26, no. 3, pp. 393-404, Mar, 2007.